Chinese Journal of Chemical Engineering 27 (2019) 314–321

Contents lists available at ScienceDirect

Chinese Journal of Chemical Engineering

journal homepage: www.elsevier.com/locate/CJChE

Article

Performance investigation of Fe_3O_4 blended poly (vinylidene fluoride) membrane on filtration and benzyl alcohol oxidation: Evaluation of sufficiency for catalytic reactors

Huseyin Gumus

Bilecik Seyh Edebali University, Osmaneli Junior Technical College, Bilecik 11500, Turkey

ARTICLE INFO

Article history:
Received 20 January 2018
Received in revised form 24 April 2018
Accepted 1 May 2018
Available online 21 May 2018

Keywords:
Benzyl alcohol oxidation
Magnetic iron oxide
Polymer supported catalyst
PVDF filtration membranes

ABSTRACT

Fe_3O_4-PVDF membranes were prepared by blending of magnetic Fe_3O_4 powders with polyvinylidene fluoride to investigate whether those were usable or not in catalytic membrane reactors. Filtration performances and catalytic activity of membranes in microwave conditions were measured in separate processes. Composite Fe_3O_4-PVDF membranes were characterized by TG-DTA, FTIR, XRD, SEM and contact angle techniques. Disappearing of α-phases at PVDF was observed with increasing amount of additives from XRD diffraction patterns. Decomposition of polymer fastened due to catalytic effect of Fe_3O_4. Finger-like structures and large number of small pores were observed at the SEM images. Those provided effective transportation of substrate among the active sites of catalyst. At the experiments conducted in batch reactor, 51%, 77%, 66% and 63% benzyl alcohol conversion were recorded for 2%, 4%, 6% and 8% Fe_3O_4-PVDF composite pieces respectively. Catalyst were separated magnetically and reused several times. On the other hand Fe_3O_4 blended PVDF membranes provided improved flux and BSA rejection compared with performance of bare PVDF membrane; 41.6% BSA rejection was obtained with 4% Fe_3O_4-PVDF whereas it was only 6.7% for PVDF. Fe_3O_4-PVDF composites performed high activity for the benzyl alcohol oxidation in batch reactor and also better filtration at filtration cell. These results promise to obtain practical and low cost membrane material for catalytic reactors usable in microwave support to get fast results.

1. Introduction

Immobilization of a catalytic particle onto polymer support may add some extra improved catalytic performance to particles thanks to potentially multi phases consist of specific area, selective sorption and transferring properties of polymer structure [1,2]. Catalytic oxidations of alcohols to aldehydes or ketones are important initial steps for synthesis of fine chemicals [3]. At homogeneous synthesis route chromium (VI), permanganate, dimethyl sulfoxide and periodate were used as a catalyst and good yield was obtained [4], but some problems emerging with using mentioned reactants at stoichiometric ratio such as corrosion of reaction cup, high cost, separation and regeneration difficulty, adverse effect of toxic chemicals to environment and living, the expectations have been focused on the developing of green, protective and high yield processes [5]. As a result of increasing awareness and demand for useful reaction components and systems, solid catalyst was explored and it has been developing continuously. Support materials may improve catalyst activity beside easy separation from the reaction mixture as Min and coworkers reported that improving effect of SiO_2 for Pd catalyst [6]. Bansal *et al.* were used Cu-Ni doped complex catalyst supported with Zeolite-Y [7]. Manganese oxide combined with activated carbon was used for benzyl alcohol oxidation and other reactions thanks to its multi number oxidation states [8,9]. Ammonium molibdate salts [10], titanium dioxide [11], bare manganese oxide [12] solid catalysts also were used as heterogeneous catalyst for different kinds of applications. Even if supported catalyst materials have high activity with their very small particle size called as micro or nano structures, problems during the separation are inevitable. Controllable pore size, pore distribution and surface chemistry made polymers preferable for catalysis as support material which provide easy separation without any loss of performance [13]. PVDF which has high mechanical and chemical resistance polymer consist of 50%–70% crystal forms called as α (alpha), β (beta) and γ (gamma) mainly [14]. It was used as a support material for Fe/Pd metal catalysts couple [15].

Properties of magnetic Fe nanoparticle loaded PVDF composite capsules such as effective separation of substrate and conversion of organic waste, easy separation without solvent, reusability and low cost made polymer support advantageous and benign support materials for green synthesis prospects [16]. Fe_3O_4 anchored PVDF membranes were also prepared and used at filtration process, and it was also preferred as filtration pervaporation systems [17]. Pd/Fe-PVDF was used

E-mail address: huseyin.gumus@bilecik.edu.tr.

https://doi.org/10.1016/j.cjche.2018.05.006
1004-9541/

for trichloride acetic acid removal [18]. Fe-zeolites/PVDF and CuO-PVDF were used to oxidize benzene and benzyl alcohol with H_2O_2 [19,20]. The hydrophobic nature of PVDF facilitates easy transfer of organic phases to active sites of catalyst in addition to its supporting mission for catalyst [21]. Advantageous of catalyst embedded polymeric structures can be associated with filtration application to obtain *in-situ* production of fine chemicals during the filtration. Thus, fast and low cost processes could be developed. Different type of catalytic reactors such as photo catalytic, submerged and bioreactors are available and those are combination of filtration membranes and catalyst which provide easy reaction, quick separation and reusability [22]. To improve the yield of a reaction system, parameters such as reactant concentration, temperature, reaction time and others should be adjusted appropriately. For the filtration processes, membrane filtration properties should be evaluated in addition to catalytic performances.

In this study, preparation and characterization of magnetic Fe_3O_4 loaded PVDF composites were conducted as a candidate of green synthesis route. For the first time, filtration properties of Fe_3O_4 blended PVDF membranes were simultaneously investigated with the performances of those on benzyl alcohol oxidation to benzaldehyde in microwave assisted oxidation conditions. According to our knowledge, catalytic activity of polymer supported magnetic particles (Fe_3O_4-PVDF) for benzyl alcohol oxidation to benzaldehyde in microwave conditions was firstly reported with this study in terms of cost effective, fast and easily separable green catalyst properties. Filtration performances and alcohol oxidation activities of prepared membranes were evaluated at different test process. Encouraging results were obtained to combination of Fe_3O_4-PVDF filtration membranes in catalytic reactor systems at microwave conditions.

2. Materials and Methods

2.1. Materials

Due to its high chemical, physical and thermal durability of polyvinylidene fluoride PVDF (Solef 6010, obtained from MINGER) was used as the polymer material without any purification. *N,N*-dimethylformamide, DMF (73.09 $g\cdot mol^{-1}$, 0.944 $g\cdot ml^{-1}$ Sigma Aldrich) was used as solvent. Nonsolvent was double distilled water. For the synthesis of magnetic particles, $FeCl_2$ (126.75 $g\cdot mol^{-1}$, 98%), $FeCl_3$ (162.20 $g\cdot mol^{-1}$, 98%) and ammonium hydroxide, NH_4OH (35.05 $g\cdot mol^{-1}$, 26%, *d*: 0.91 $g\cdot ml^{-1}$) were purchased from Sigma-Aldrich. Benzyl alcohol (108 $g\cdot mol^{-1}$, 1.05 $g\cdot ml^{-1}$) and hydrogen peroxide (34.01 $g\cdot mol^{-1}$, 30% w/v) were purchased from Merck and Panreac Company. Bovine serum albumin, BSA (MW: 66000, ≥98% purity, Sigma Aldrich), was used to prepare model protein solution with boric acid, H_3BO_3 (61.83 $g\cdot mol^{-1}$, Sigma-Aldrich), phosphoric acid, H_3PO_4 (98 $g\cdot mol^{-1}$, Sigma-Aldrich) and acetic acid, CH_3COOH (60.05 $g\cdot mol^{-1}$, 99.7%, Sigma-Aldrich) as pH adjustment chemicals.

2.2. Preparation of magnetic Fe_3O_4 and Fe_3O_4-PVDF membranes

Preparation of magnetic Fe_3O_4 was conducted as reported by Mandel *et al.* [23]. A mixture of Fe (II) and Fe (III) 1:2-mol ratio was prepared. Solution was heated to 70 –80 °C. Until to pH: 12, ammonium hydroxide was added. Black precipitates were separated by magnet and dried at 60 °C for 6 h. To obtain Fe_3O_4-PVDF, Fe_3O_4 and PVDF (1.6 g in 10-ml DMF) solutions were prepared at separate cups. Then Fe_3O_4 in DMF according to 0%, 2%, 4%, 6%, 8% mass ratio was added to PVDF solution at 50 °C (Table 1). Before addition Fe_3O_4 solution was waited in ultrasonic bath during 10 min to provide homogeneous dispersion. The mixture of PVDF/DMF/Fe_3O_4 was stirred at 250 $r\cdot min^{-1}$ at 65 °C for 12 h to provide homogeneous dispersion of particles. Dope solution was waited for 10 min to avoid air bubbles during the process and casted on to glass plate (15 cm × 15 cm). It was spread to surface uniformly by casting knife with a knife gap of 300 μm at 25 °C. After exposure to air for 25 s, the glass plate was quickly immersed into distilled water bath. Another water cup was used to keep the temperature in balance. Representative illustration of preparation was given at Fig. 1. Membranes prepared by phase inversion were dried and used for characterization and oxidation experiments. Filtration membranes were stored in distilled water until the filtration experiments. Prepared PVDF-metal oxide composites contain 0%, 2%, 4%, 6%, 8% Fe_3O_4 mass ratio were defined as PVDF, F2-P, F4-P, F6-P and F8-P respectively.

Table 1
Conversion and benzaldehyde selectivity of Fe_3O_4-PVDF samples

Sample	DMF/%	PVDF/%	Fe_3O_4/%
PVDF	14	86	–
F2-P	14	82	2
F4-P	14	80	4
F6-P	14	78	6
F8-P	14	76	8

2.3. Characterization of Fe_3O_4 and Fe_3O_4-PVDF membranes

Samples were analyzed by XRD (Rigaku 2000) to understand crystal structure of composites and powder, at 2θ:2°–70° with 2 (°)·min^{-1} scanning speed. Perkin Elmer FTIR over a range of 4000–400 cm^{-1} was used to analyze functional groups and Seiko Exstar 7200 thermal analyzer (TG and DTA) was used to measure thermal stability of samples. The morphologies were examined by scanning electron microscopy at 10 kV (Carl Zeiss ULTRA Plus). Membranes were firstly broken in liquid nitrogen, and cross-section images were photographed. The surface wettability and hydrophilicity of membranes was investigated by static contact angle analyzer (KSV Attention, Finland) at room temperature. Sessile drop method was used, and average value was calculated by at least four different measurements of each membranes. Germany). Gas chromatography with HP5 column (Agilent 6890) was used for analysis of organics. One microliter of mixture was injected, and it was analyzed at 100 °C (5 min wait), 180 °C (5 min wait) and 220 °C (2 min wait). Concentration of BSA used as a model pollutant to determination of rejection performances of membranes. It was measured by UV–visible spectrometer (PG instruments, T80) at 280-nm wavelength.

To determine water uptake capacity (WU), membranes stored in water were weighted (W_w) after mopping slightly with blotting paper. Wet membranes were dried in 40-°C vacuum oven for 2 h, and dry membranes were weighted (W_d). By using wet and dry masses of membranes, water uptake capacities were calculated by Eq. (1).

$$WU = \frac{W_w - W_d}{W_w} \times 100\% \quad (1)$$

Membrane porosity (PO) was calculated by mass of wet and dry membranes [21,28]. Following Eq. (2) was used for porosity calculation.

$$PO = \frac{W_w - W_d}{dA\delta} \times 100\% \quad (2)$$

where *d* is the density of water used at 25 °C; *A* is membrane area in wet state (cm^2), and δ is the thickness of membrane in wet form (cm).

2.4. Pure water flux, protein rejection and antifouling performances of membranes

Pure water permeability (PWP) of prepared membranes was measured by collecting permeated distilled water ($L\cdot m^{-2}\cdot h^{-1}$) at ultra-filtration cross-flow membrane cell. Transmembrane pressures

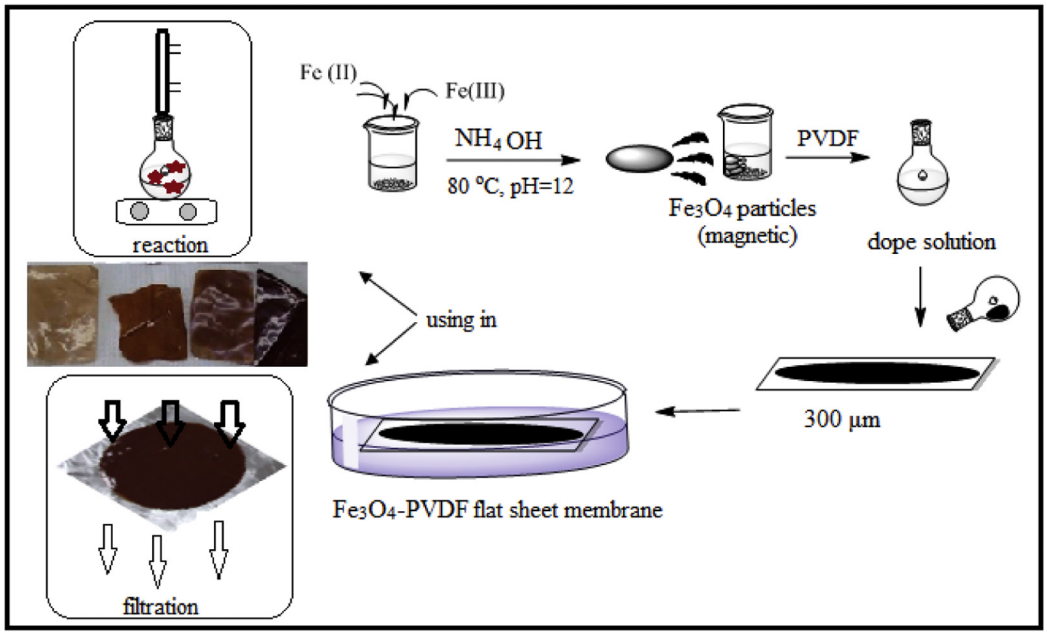

Fig. 1. Preparation steps of Fe_3O_4 and Fe_3O_4-PVDF.

(TMP) were adjusted as 200 kPa after pre-conditioned of membranes for 1–3 h. PWP was calculated by Eq. (3).

$$\mathrm{PWP} = \frac{V}{At} \tag{3}$$

where V is volume of permeate (L); A is membrane area in square meter (1.7×10^{-3} m^2), and Δt is the sampling time (h). Compaction factor (CF) was calculated to get information about physical resistance of membranes by dividing of initial PWP value to constant PWP value. BSA was used as a model pollutant to understand rejection performances of membranes. For this 0.5 $g \cdot L^{-1}$ aqueous BSA solution was prepared with phosphate buffer solution (0.01 $mol \cdot L^{-1}$, pH:7.4) and filtered at 200 kPa. Permeate was collected and BSA concentration was measured by UV-spectrophotometer, and rejection capacity was calculated by Eq. (4).

$$\mathrm{BSA} = \left(1 - \frac{C_p}{C_f}\right) x100\% \tag{4}$$

where C_p and C_f are the concentration of protein in permeate and feed solutions respectively. After BSA filtrated membranes were washed, they were immersed in distilled water for 20 min. Then PWP values of cleaned membranes were measured. Flux recovery percentages of membranes (FRR) were calculated by Eq. (5).

$$\mathrm{FRR} = \left(\frac{\mathrm{PWP}_2}{\mathrm{PWP}_1}\right) \times 100\% \tag{5}$$

where PWP_1 is pure water flux values of membrane before BSA filtration, and PWP_2 is the pure water flux of BSA rejected and cleaned membrane. The thickness of the dried and wet membranes was tested by thickness measuring instrument (Hornbach, 0.25 mm to 0.01 mm range).

2.5. Catalytic activity experiments

Catalytic activities of Fe_3O_4 and Fe_3O_4-PVDF were investigated under the conditions of batch reactor. Before using, 0.02 g Fe_3O_4-PVDF membrane pieces (1.5 cm × 1.5 cm) were kept in benzyl alcohol for 1 h at room temperature to provide sufficient diffusion of substrate inside the membrane pores. Catalytic pieces were put in to 50-ml flask with 1-mmol benzyl alcohol and 1-mmol H_2O_2. Mixture was placed to microwave oven powered 500 W for 8 min. Sample taken by micro syringe was analyzed with GC (without any filtration). Catalytic pieces were washed with acetone and pure water. They were reused there times after dried. Catalytic activity of samples was reported as conversion and benzaldehyde selectivity according to following Eqs. (6) and (7) [8]. Powder Fe_3O_4 was used as a catalyst at the same reaction conditions of Fe_3O_4-PVDF. Sample taken from powder catalyst was filtered by syringe filter before injection to column.

$$C = \frac{C_{\mathrm{alcohol(initial)}} - C_{\mathrm{alcohol(final)}}}{C_{\mathrm{alcohol(initial)}}} \times 100\% \tag{6}$$

$$S = \frac{\text{Amount of benzaldhyde}}{\text{Amount of all products}} \times 100\% \tag{7}$$

3. Results and Discussion

3.1. Fe_3O_4 and Fe_3O_4-PVDF characterization

The X-ray diffraction patterns of Fe_3O_4 and Fe_3O_4-PVDF were shown in Fig. 2. Diffraction peaks observed at 2θ = 30.1°, 35.4°, 43.2°, 56.9° and 62.6° indicated to presence of magnetite form Fe_3O_4 [25,26]. Fe (0) structures also could be seen by the broad peaks at around 44.6°–44.7° due to poor crystallinity of particles [24]. Presence of Fe_3O_4 peaks in XRD patterns of Fe_3O_4-PVDF sample were a good evidence for the interaction of Fe_3O_4 and PVDF which is important for structural durability of catalyst. Increasing amount of Fe_3O_4 addition to polymer resulted in shift on 2θ position of Fe_3O_4. New peaks at 20.4 (for F2-P) and 20.7° (for F8-P) with very small intensity corresponded to emerging of β-phase PVDF while peaks of α-phase PVDF at 2θ = 19°, 19.6°, 20.1° and 25.4° partially disappeared [14]. Amorphous structure formation increased for polymer due to agglomeration and tightening effect of particles after addition of Fe_3O_4.

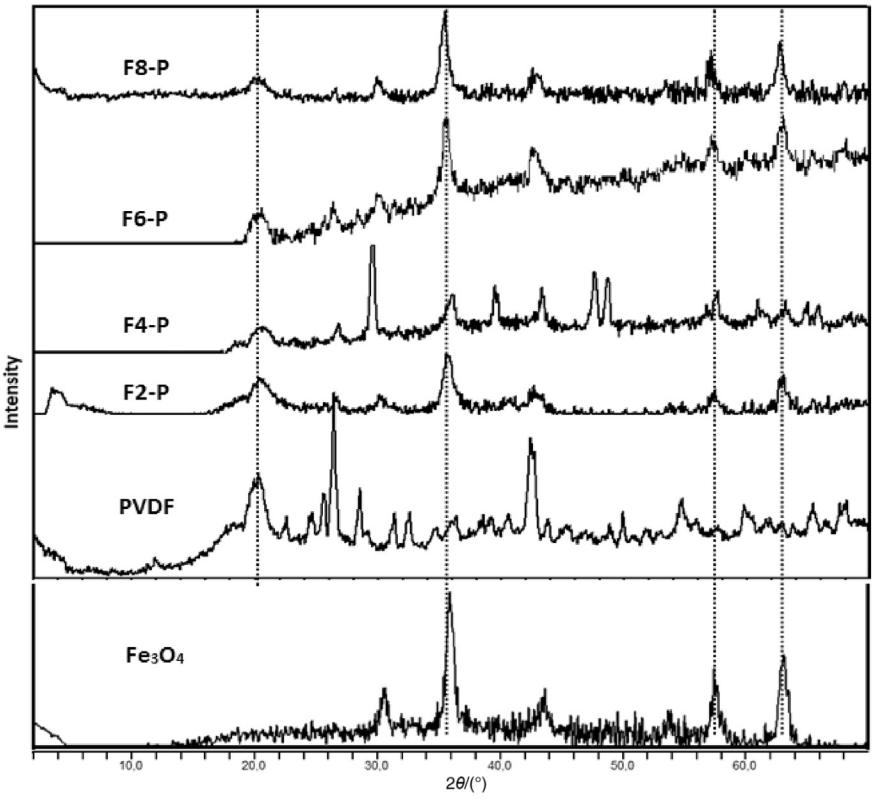

Fig. 2. XRD patterns of samples.

Effect of Fe_3O_4 on PVDF structure has been investigated by FT-IR analysis (Fig. 3). The bands at around 580–590 cm^{-1} corresponded to Fe—O stretching vibration, 1620 cm^{-1} was adsorbed H—O—H vibration of iron oxide [27]. The bands at 1122, 1046 and 977 cm^{-1} represented to complex structures of FeO and FeOH with water molecules [28]. CH and CF_2 bond stretching vibrations of PVDF were observed at 1403 and 877–1175 cm^{-1} respectively. CF stretching vibration corresponded to 1070 cm^{-1}, and it has not changed for composites. α-Phases of PVDF could be understood by 761, 796 and 975 cm^{-1} bands. The bands at around 838–840 cm^{-1} with 1273 and 1431 cm^{-1} confirmed the presence of α and β-phases as determined by XRD results. After the Fe_3O_4 addition, intensity of 797 cm^{-1} and 975 cm^{-1} bands of PVDF increased. But, intensity of 761, 797 and 975 cm^{-1} bands of F4-P decreased. That means α-phases of PVDF became amorphous. The changes of bands at around 700–650 cm^{-1} with increased Fe_3O_4 may be attributed to hydrogen bonding between OH groups of Fe_3O_4 and fluoride of PVDF chain [29].

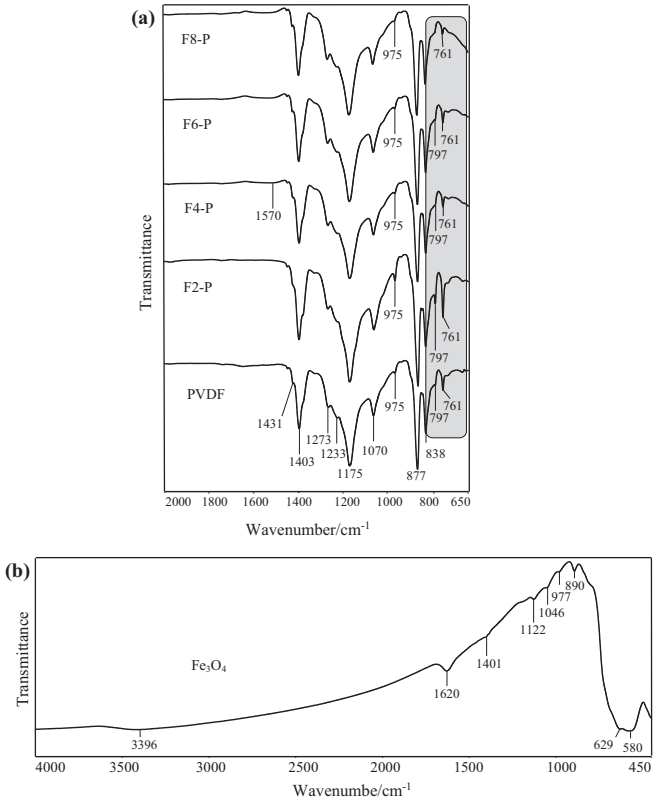

Fig. 3. FT-IR spectra of Fe_3O_4 (a) and PVDF samples (b).

Thermal decomposition of PVDF completed at three stages with temperature ranges 395–485 (with 2.5%–60% mass loss), 485–590 °C and 600–1000 °C as demonstrated at Fig. 4. Different ash contents obtained for the PVDF, F2-P, F4-P, F6-P and F8-P samples were due to the inclusion of solvent during the calculation of dope solution, but burning only polymer and additives with small amount of solvent at the thermal analyzer. After exposing the samples to heat, remaining weight indicated to Fe_3O_4 inside membranes. All of the organic contents of Fe_3O_4 embedded composites were burned. Decomposition of polymer started with breaking of CH and CF bonds and progressed by mass loss. Decomposition of PVDF hastened especially at the initial steps of decomposition with the Fe_3O_4 addition. Onset temperature F8-P was recorded as 284 °C while it was 374 °C for raw PVDF. From the results, it was concluded that due to catalytic effect of Fe_3O_4, decomposition of polymeric matrix induced and onset temperature decreased. Exothermic DTA curves formed during the burning of organic structure were seen at lower temperatures compared with DTA curves of PVDF with increased Fe_3O_4 ratio. On the other hand t_{max} values which is the max decomposition temperatures of F4-P, F6-P and F8-P were higher than of raw PVDF although catalytic activity of Fe_3O_4. Those were recorded as 470, 471, 484, 486 and 482 for PVDF, F2-P, F4-P, F6-P and

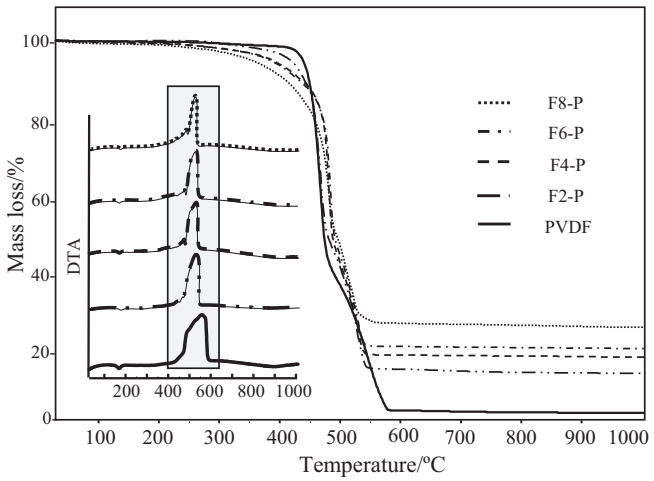

Fig. 4. TG curves of samples.

F8-P respectively. That may be due to two reasons: (I) protecting effect of well dispersed particles in the polymer or (II) formation of different iron oxide species by oxygen releasing [30]. Burning of organic substance was completed at 600 °C for all samples. Residues observed for composite samples were higher than expected for their contents such as, approximately 30% for F8-P and 19% for F4-P. Those results proved the evidence of catalytic activity of Fe_3O_4 at the initial steps of burning and preventing effect of Fe_3O_4 after the initial steps.

Cross-section SEM images of Fe_3O_4-PVDF samples were presented in Fig. 5. Sponge-like structure of PVDF reshaped, and finger-like channels formed after Fe_3O_4 addition. Two percent and 4% ratio of Fe_3O_4 addition resulted in appropriate holes whereas with increasing amount of Fe_3O_4 (6% and further), agglomerated structures and particles began to be seen on the membrane. As a result of high amount of Fe_3O_4 loading, polymer structure became pressed and shrunk. Magnetic property of powder was also one of the effective parameters on the regulation of structure. Agglomeration of particles accelerated with magnetism. Effect of Fe_3O_4 amount could be understood by porosity and thickness results of flat sheet Fe_3O_4-PVDF structures measured according to overall porosity measurement procedures [31]. Porosity values firstly increased then decreased gradually with increased amounts of Fe_3O_4, as expected (Fig. 6). Those were recorded as 49.2%, 56%, 71.3%, 72.6% and 62.1% for PVDF, F2-P, F4-P, F6-P and F8-P respectively. By considering the characterization results, composites of containing 4% and 6% Fe_3O_4 could be presumed as the optimum compositions due to their high porosity. Although there were no exact changes for thicknesses of samples, intense structures formed with increasing Fe_3O_4 loading. Thickness values were obtained as 65, 60, 61, 66 and 62 μm respectively for the samples of the series. PVDF membrane has thicker structure compared with 2%, 4% and 8% Fe_3O_4 containing samples. It was due to easy phase separation of polymer absence of interacted Fe_3O_4 particles. Furthermore electrostatic interaction at around PVDF chain resulted in

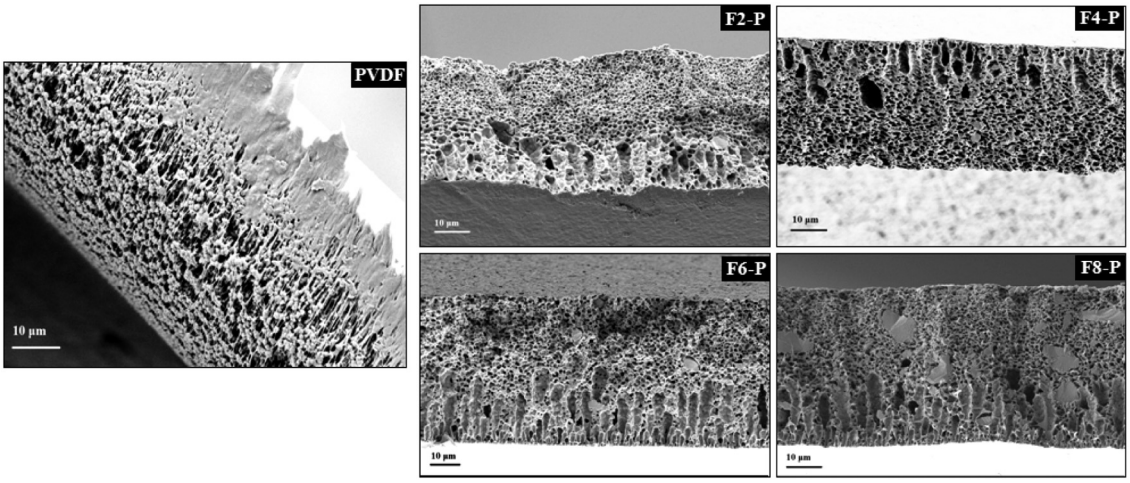

Fig. 5. SEM images of samples.

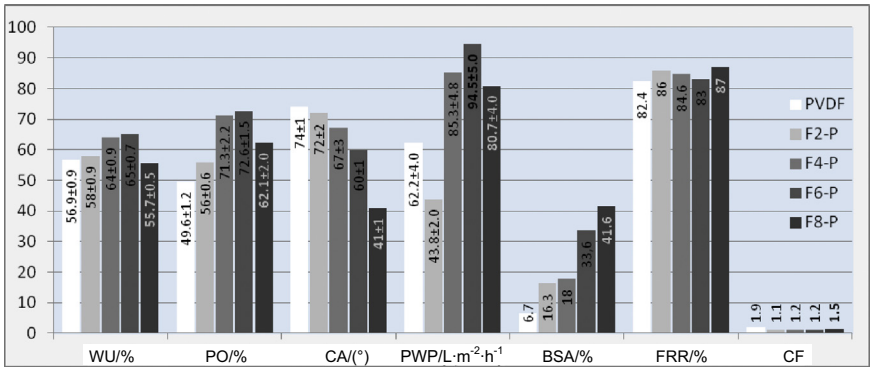

Fig. 6. Filtration properties of PVDF and Fe_3O_4-PVDF samples. WU: Water uptake, PO: Porosity, CA: Contact angle, PWP: Pure water permeability, BSA: Bovine serum albumin (rejection), FRR: Flux recovery ratio, CF: Compaction factor.

swollen structure which has thicker cross-section. Fe_3O_4 added samples gained pressed structure due to interaction between PVDF chain and Fe_3O_4. Thickest structure of F6-P was due to favorable spreading of particles on the polymeric surface as could be seen from the porosity values. However structure was pressed and thickness decreased when the Fe_3O_4 was 8%.

3.2. Filtration performances of membranes

Water permeability, BSA rejection performance as a model contaminant and other properties of membranes were tested by cross-flow filtration system, and results were presented in Fig. 6. Increased PWP values were obtained with F4-P and F6-P, while PWP decreased for further additive although gradually decreased contact angle of F8-P which showed increasing hydrophilicity. Water permeation is not only depends on hydrophilicity but also porosity, thickness and water uptake [32]. Highest porosity and water uptake were recorded as 72.6% and 65% for F6-P. Porosity and water uptake values of membranes were higher than that of pristine PVDF membrane. A relation had been observed between thickness and pore size of membranes with permeation behaviors of those. Large amount of small pores formed during the phase separation as a result of accelerated water-solvent separation process due to hydrophilic metal oxide additives. Those were seen as increase in porosity, water uptake and hydrophilicity. Decreased WU%, PO% and PWP results revealed that 8% addition amount resulted in adverse effect for transferring of water among channels. Advantage of high amount of additive was seen at the BSA rejection results; 41.6% rejection was recorded with F8-P whereas it was only 6.7% for PVDF. Suppressed and blocked pores provided improved BSA rejection. Thickened structure had a significant effect on rejection performance of membranes in addition to small pores formed during the instant phase separation. Lower compaction values of composite membranes compared with PVDF confirmed to increase in viscosity of dope solution. That indicated to thicker skins by increased additive. Due to permeable polymeric lumps observed in SEM images of PVDF (Fig. 5), low rejection but moderate flux was obtained. Flux of BSA filtrated membranes were investigated and FRR% values were obtained. It was known that contaminant accumulation on the surface of membrane occurs by electrostatic interaction [33]. Highest flux recovery was recorded with F8-P as 87%. That was due to small pores which prevent entering the organic molecules into channels and hydrophilicity which hinders accumulation of BSA on the surface of membrane. FRR values of samples slightly increased with increased hydrophilicity. That may be explained by relation between hydrophilicity and roughness of surface. High amount of additive provides good hydrophilicity and high roughness. Due to particles tend to accumulate easily in rough surfaces; roughness and hydrophilicity should be improved simultaneously to obtain more resistive antifouling membranes. Composites prepared by Fe_3O_4 addition performed higher filtration and rejection performances than PVDF membrane.

3.3. Catalytic activity of Fe_3O_4 and Fe_3O_4–PVDF

Catalytic activity measurements of Fe_3O_4-PVDF for benzyl alcohol oxidation were conducted in a round bottom flask; 1:1-mol ratio alcohol:peroxide and 0.06 g catalyst were adjusted as reactants. Reaction cup was fixed to microwave furnace to adaptation of advantages of microwave radiation. It was refluxed with a condenser with solvent free conditions. Optimized reaction conditions were presented at Table 2.

High yield was obtained when the catalyst amount and Fe_3O_4 ratio increased. That was directly related to large amount of active sites of catalyst. Performance of composite was affected by Fe_3O_4 amount added to PVDF. Large holes induced easy transferring of substrates while narrowing of structure consequently suppressed the pores and that caused hurdled transferring of substrates to active sites. That decreased the conversion as could be seen from conversion results of F8-P. Although decreasing porosity with high Fe_3O_4 amount (Section 3.1), moderate conversion and selectivity was obtained with F8-P. That may be attributed to favorable pore dispersion. Catalyst amount was seen that it has a direct effect on product type. High benzaldehyde selectivity and conversion were obtained when the Fe_3O_4-PVDF was 0.02 g, but selectivity decreased when it was 0.04 g and further amounts. That meant benzaldehyde was converted to over oxidation products such as benzoic acid. Another important parameter investigated in this study which effected conversion and selectivity of benzyl alcohol was alcohol:peroxide ratio. Different conversion and selectivity results were presented about alcohol:peroxide effect in literature [34,35]. It should be considered that organic structure facilitated substrate transportation; on the other hand, hydrophilic groups easily interact with water and peroxide. Either hydrophilicity or hydrophobicity of structure became dominant, and water or organic substrate transportation increased. Fe_3O_4-PVDF performed high conversion but low selectivity when used without peroxide (49% and 6% respectively). When the peroxide:alcohol ratio was 0.2, conversion and selectivity were approximately equal. Highest selectivity and conversion were recorded with the alcohol:peroxide ratio of 0.8 and 1.5 respectively. The reasons may be: (1) stoichiometrically scarcity of peroxide amount, (2) transferring problems of peroxide to active sites of catalyst due to interaction of peroxide with polymer, (3) peroxide decomposition on active sites of catalyst. Complex peroxy-metal structures formed as a result of interaction of hydrogen peroxide and metals on catalyst during the oxidation. This semi product reacted with benzyl alcohol and benzaldehyde formed. But in the presence of large amount of catalyst, peroxide decomposed quickly. Eighty-nine percent conversion was obtained at 700 W (Table 2). Low benzaldehyde selectivity was observed at high microwave power due to decomposition of peroxide.

Fe_3O_4-PVDF pieces were separated from mixture with a magnet and washed with acetone then reused three times. Surprisingly, particles performed higher conversion than first circle but little selectivity. Microwave radiation may shrink the transportation channel of polymeric support. With ongoing usage, benzyl alcohol conversion and benzaldehyde

Table 2
Conversion and benzaldehyde selectivity of Fe_3O_4-PVDF samples

Entry	Catalyst (amount/g)	Temperature/°C	Reaction time	Conversion–selectivity/%
1	–	R.T.	4 h	–
2	–	80	4 h	–
3	–	80①	8 min	–
4	Fe_3O_4 (0.06)	R.T.	4 h	–
5	Fe_3O_4 (0.06)	80	4 h	26.2–33.5
6	Fe_3O_4 (0.06)	80①	8 min	86.0–4.4
7	2%-Fe_3O_4-P (0.06)	R.T.	4 h	–
8	2%-Fe_3O_4-P (0.06)	80	4 h	52.6–41
9	2%-Fe_3O_4-P (0.06)	80①	8 min	51–5.35
10	4%-Fe_3O_4-P (0.06)	80①	8 min	77–15
11	6%-Fe_3O_4-P (0.06)	80①	8 min	66–17
12	8%-Fe_3O_4-P (0.06)	80①	8 min	63–35
13	8%-Fe_3O_4-P (0.02)	80①	8 min	52.6–41.6
14	8%-Fe_3O_4-P (0.04)	80①	8 min	80–8.3
15	8%-Fe_3O_4-P (0.08)	80①	8 min	80.5–9
16②0	8%-Fe_3O_4-P (0.02)	80①	8 min	49.5–6
17②0.2	8%-Fe_3O_4-P (0.02)	80①	8 min	46.5–47.7
18②0.4	8%-Fe_3O_4-P (0.02)	80①	8 min	70.3–17.11
19②0.6	8%-Fe_3O_4-P (0.02)	80①	8 min	54.6–33
20②0.8	8%-Fe_3O_4-P (0.02)	80①	8 min	37.1–66.4
21②1	8%-Fe_3O_4-P (0.02)	80①	8 min	63.2–32.5
22②1.5	8%-Fe_3O_4-P (0.02)	80①	8 min	89–7.7
23–300 W	8%-Fe_3O_4-P (0.02)	80①	8 min	3.4–7
24–700 W	8%-Fe_3O_4-P (0.02)	80①	8 min	89.4–5.5
2. reuse	8%-Fe_3O_4-P (0.02)	80①	8 min	98.3–1.82
3. reuse	8%-Fe_3O_4-P (0.02)	80①	8 min	99.2–4.39
4. reuse	8%-Fe_3O_4-P (0.02)	80①	8 min	98.1–5.5

Note: Reaction was carried out in 50 ml flask with condenser in 500 W microwave, 1 mmol H_2O_2 and 1 mmol benzyl alcohol ratio unless otherwise stated. Mixture was analyzed with HP-5 column by GC.
① In microwave radiation.
② H_2O_2:Benzyl alcohol ratio (mol).

selectivity increased gradually. Because of sufficient diffusion of organic substrate inside polymeric channels facilitated to transportation of substrate to active sites of iron oxide catalyst at ongoing usages. Good interaction between benzyl alcohol and iron oxide species resulted in increased conversion. Metal concentration in the reaction solution was analyzed with atomic absorption (Perkin Elmer, PinAAcle 900 F). After the fourth reuse, iron concentration was determined as 5.217 $mg \cdot L^{-1}$ ($R^2 = 0.999931$). Any iron remnant had not been observed after first using of catalyst. After repeating reuse metal leaching increased due to effect of deformation of microwave and solvent.

Small amount of Fe_3O_4-PVDF catalyst has benefits of easy usage and low cost catalytic activity. When compared with other catalyst (Table 3), moderate activity was obtained with Fe_3O_4-PVDF composites at solvent free area. Also easy separation from reaction media without solvent and reusability were concluded as advantageous for oxidation reactions. Microwave conditions provided new aspect to the polymer supported catalyst and catalysis system carried out in this study.

Table 3
Comparison of catalytic activity of Fe_3O_4-PVDF with other catalyst in literature

Catalyst type and amount	Operating conditions	Reaction time	Conversion and selectivity/%	Refs.
Fe_3O_4-AA-Pd, 0.03 g	Substrate: BzOH, 2 mmol; Oxidant: O_2; Solvent: No solvent; Temp.: 50 °C	1.5 h	98–48	[25]
PVP-HPA, 0.15 g	Substrate: BzOH, 5 mmol; Oxidant: H_2O_2, 6 mmol; Solvent: No solvent; Temp.: 90 °C	2 h	86–100	[37]
Ag-Pb/SPES, 2.4 $mg \cdot cm^{-2}$	Substrate: BzOH, 5 mmol; Oxidant: H_2O_2, 50 ml and 1.5 $ml \cdot min^{-1}$ circulation; Solvent: No solvent; Temp.: 70 °C	1 h	97–95	[36]
Fe(0)/FeO-PVDF, 0.5 g	Substrate: methylene blue, 100 $mg \cdot L^{-1}$; Oxidant: H_2O_2, 5 ml; Solvent: No solvent; Temp.: 25 °C	–	80 $mg \cdot g^{-1}$	[38]
Pd/Fe-PVDF-Al_2O_3, 2.04 mg	Substrate: MCAA, 5 $mg \cdot L^{-1}$; Solvent: water; Temp.: 25 °C	0.5 h	98.7	[15]
Fe-Zeolite/PVDF, 0.5 g	Substrate: Benzene, 100 ml; Oxidant: H_2O_2, 12.5 mmol; Solvent: Acetone; Temp.: 35–50 °C	10 min	97–63	[20]
PVDF membrane	Substrate: BzOH; Oxidant: H_2O_2; Solvent: water	–	98.4–47.9	[21]
CuO-PVDF, 16 %	Substrate: Benzene, 2.4 $g \cdot L^{-1}$; Oxidant: H_2O_2,1/1 Benzene; Solvent: acetonitrile; Temp.: 35 °C	19.4 s	−2.3	[19]
$(NH_4)_6Mo_7O_{24}$, 4 mmol	Substrate: BzOH,200 mmol; Oxidant: H_2O_2,199 mmol; Solvent: 15 ml water; Temp.: 60–80 °C	4 h	98–74	[2]
NH_4Mo/PVDF capsule, 0.85 mmol	Substrate: BzOH, 9.26 mmol; Oxidant: H_2O_2, 9.20 mmol; Solvent: acetonitrile; Temp.: 90 °C	4 h	99.1–56	[39]
Cu(II)-APS, 0.03 g	Substrate: Styrene-BzOH,5 mmol; Oxidant: TBHP and others, 10 mmol; Solvent: water; Temp.: 60 °C	8 h	−96	[1]
8% Fe_3O_4-PVDF, flat membrane	Substrate: BzOH, 1 mmol; Oxidant: H_2O_2, 1 mmol; Solvent: No solvent; Temp.②: 60–90 °C②	8 min	98.4–66.4①	in this study

Note: BzOH: Benzyl alcohol.
① Independent data.
② Microwave conditions.

4. Conclusions

Fe_3O_4 blended PVDF composites were prepared and tested in filtration cell and benzyl alcohol oxidation reaction. To obtain fast, easy and low cost *in-situ* production the combination of samples in catalytic membrane reactor systems with microwave radiation was investigated. From the characterization it was concluded that with increasing Fe_3O_4 α-phase of PVDF turned to amorphous form. Thermal decomposition of polymer fastened due to catalytic effect of Fe_3O_4.Initial decomposition temperature of organics decreased, while Fe_3O_4 acted as a retardant at further stages. Higher t_{max} values attributed to protecting behavior of additive were observed such as 482 and 486 for F4-P and F2-P respectively compared with pristine PVDF (470 °C). From the SEM analysis, finger-like channels were observed for composites. Increased porosity, water flux and BSA rejection were obtained with Fe_3O_4-PVDF composite membranes. Fe_3O_4-PVDF membranes tested for benzyl alcohol oxidation in batch system at microwave conditions provided better alcohol conversion and selectivity compared with the yield of powder Fe_3O_4. Optimum conversion and selectivity were achieved with 0.02 g of F8-P. Small amount of 8% Fe_3O_4 contained catalyst were agreed as favorable for green synthesis. In addition to catalytic activity, Fe_3O_4-PVDF membranes performed improved filtration and rejection compared with bare PVDF. Rejection increased to 41.6% from 6.7% for F8-P relatively with increasing flux to 94.5 $L \cdot m^{-2} \cdot h^{-1}$ PWP.

By considering the filtration and catalytic activity of durable Fe_3O_4-PVDF membranes, it was concluded that those membranes could serve as a component of catalytic membrane reactor combined with microwave radiation. These findings have potential to induce new designs using mentioned fragments for featured systems.

Acknowledgements

We would like to thank Chemistry Department of Bilecik Seyh Edebali University for their supports providing the facilities of laboratory equipment.

References

[1] S.M. Islam, A.S. Roy, P. Mondal, S. Paul, N. Salam, A recyclable polymer anchored copper(II) catalyst for oxidation reaction of olefins and alcohols with *tert*-butylhydroperoxide in aqueous medium, *Inorg. Chem. Commun.* 24 (2012) 170–176.
[2] M.G. Buonomenna, A. Figoli, I. Spezzano, M. Davoli, E. Drioli, New PVDF microcapsules for application in catalysis, *Appl. Catal. B Environ.* 80 (2008) 185–194.
[3] N. Dimitratos, J.A. Lopez-Sanchez, D. Morgan, A. Carley, L. Prati, G.J. Hutchings, Solvent free liquid phase oxidation of benzyl alcohol using Au supported catalysts prepared using a sol immobilization technique, *Catal. Today* 122 (2007) 317–324.
[4] H. Guo, M. Kemell, A. Al-Hunaiti, S. Rautiainen, M. Leskelä, T. Repo, Gold-palladium supported on porous steel fiber matrix: structured catalyst for benzyl alcohol oxidation and benzyl amine oxidation, *Catal. Commun.* 12 (2011) 1260–1264.
[5] A. Kamimura, H. Komatsu, T. Moriyama, Y. Nozaki, Sub-stoichiometric oxidation of benzylic alcohols with commercially available activated MnO_2 under oxygen atmosphere: a green modification of the benzylic oxidation, *Tetrahedron* 69 (2013) 5968–5972.
[6] B.K. Min, A.K. Santra, D.W. Goodman, Understanding silica-supported metal catalysts: Pd/silica as a case study, *Catal. Today* 85 (2003) 113–124.
[7] V.K. Bansal, P.P. Thankachan, R. Prasad, Oxidation of benzyl alcohol and styrene using H_2O_2 catalyzed by tetraazamacrocycle complexes of Cu(II) and Ni(II) encapsulated in zeolite-Y, *Appl. Catal. A Gen.* 381 (2010) 8–17.
[8] Q. Tang, X. Huang, Y. Chen, T. Liu, Y. Yang, Characterization and catalytic application of highly dispersed manganese oxides supported on activated carbon, *J. Mol. Catal. A Chem.* 301 (2009) 24–30.
[9] B. Eren, H. Gumus, Copper doped K-birnessite as an efficient catalyst for the synthesis of 2-aryl benzimidazoles, *React. Kinet. Mech. Catal.* 114 (2015) 571–582.
[10] M.P. Chaudhari, S.B. Sawant, Kinetics of heterogeneous oxidation of benzyl alcohol with hydrogen peroxide, *Chem. Eng. J.* 106 (2005) 111–118.
[11] R.A. Damodar, S.J. You, H.H. Chou, Study the self cleaning, antibacterial and photocatalytic properties of TiO_2 entrapped PVDF membranes, *J. Hazard. Mater.* 172 (2009) 1321–1328.

[12] S.H. Do, B. Batchelor, H.K. Lee, S.H. Kong, Hydrogen peroxide decomposition on manganese oxide (pyrolusite): kinetics, intermediates, and mechanism, *Chemosphere* 75 (2009) 8–12.
[13] L.Y. Ng, A.W. Mohammad, C.P. Leo, N. Hilal, Polymeric membranes incorporated with metal/metal oxide nanoparticles: a comprehensive review, *Desalination* 308 (2013) 15–33.
[14] D.R. Dillon, K.K. Tenneti, C.Y. Li, F.K. Ko, I. Sics, B.S. Hsiao, On the structure and morphology of polyvinylidene fluoride-nanoclay nanocomposites, *Polymer* 47 (2006) 1678–1688.
[15] Z. Meng, H. Liu, Y. Liu, J. Zhang, S. Yu, F. Cui, N. Ren, J. Ma, Preparation and characterization of Pd/Fe bimetallic nanoparticles immobilized in PVDF·Al_2O_3 membrane for dechlorination of monochloroacetic acid, *J. Membr. Sci.* 372 (2011) 165–171.
[16] X. Zhao, L. Lv, B. Pan, W. Zhang, S. Zhang, Q. Zhang, Polymer-supported nanocomposites for environmental application: A review, *Chem. Eng. J.* 170 (2011) 381–394.
[17] Z.Q. Huang, F. Zheng, Z. Zhang, H.T. Xu, K.M. Zhou, The performance of the PVDF-Fe_3O_4 ultrafiltration membrane and the effect of a parallel magnetic field used during the membrane formation, *Desalination* 292 (2012) 64–72.
[18] X. Wang, J. Yang, M. Zhu, F. Li, Characterization and regeneration of Pd/Fe nanoparticles immobilized in modified PVDF membrane, *J. Taiwan Inst. Chem. Eng.* 44 (2013) 386–392.
[19] R. Molinari, T. Poerio, P. Argurio, Liquid-phase oxidation of benzene to phenol using CuO catalytic polymeric membranes, *Desalination* 241 (2009) 22–28.
[20] R. Molinari, T. Poerio, T. Granato, A. Katovic, Fe-zeolites filled in PVDF membranes in the selective oxidation of benzene to phenol, *Microporous Mesoporous Mater.* 129 (2010) 136–143.
[21] M.G. Buonomenna, G. Golemme, A. Figoli, E. Drioli, Fluorinated membranes as interfaces for application in catalysis, *Desalination* 250 (2010) 1147–1149.
[22] Y.H. Teow, A.L. Ahmad, J.K. Lim, B.S. Ooi, Preparation and characterization of PVDF/TiO_2 mixed matrix membrane via in situ colloidal precipitation method, *Desalination* 295 (2012) 61–69.
[23] K. Mandel, F. Hutter, C. Gellermann, G. Sextl, Synthesis and stabilisation of superparamagnetic iron oxide nanoparticle dispersions, *Colloids Surf. A Physicochem. Eng. Asp.* 390 (2011) 173–178.
[24] L. Liu, F. Chen, F. Yang, Stable photocatalytic activity of immobilized Fe_0/TiO_2/ACF on composite membrane in degradation of 2,4-dichlorophenol, *Sep. Purif. Technol.* 70 (2009) 173–178.
[25] Y.C. Dong, R.G. Ma, M. Jun Hu, H. Cheng, C.K. Tsang, Q.D. Yang, Y. Yang Li, J.A. Zapien, Scalable synthesis of Fe_3O_4 nanoparticles anchored on graphene as a high-performance anode for lithium ion batteries, *J. Solid State Chem.* 201 (2013) 330–337.
[26] F. Zamani, S. Mohsen, Palladium nanoparticles supported on Fe_3O_4/amino acid nanocomposite: highly active magnetic catalyst for solvent-free aerobic oxidation of alcohols, *Catal. Commun.* 43 (2014) 164–168.
[27] T. Xin, M. Ma, H. Zhang, J. Gu, S. Wang, M. Liu, Q. Zhang, A facile approach for the synthesis of magnetic separable Fe_3O_4@TiO_2, core-shell nanocomposites as highly recyclable photocatalysts, *Appl. Surf. Sci.* 288 (2014) 51–59.
[28] R. Jamshidi Gohari, W.J. Lau, T. Matsuura, A.F. Ismail, Fabrication and characterization of novel PES/Fe-Mn binary oxide UF mixed matrix membrane for adsorptive removal of As(III) from contaminated water solution, *Sep. Purif. Technol.* 118 (2013) 64–72.
[29] M. Abd, E. Aleem, A. Ali, Synthesis of pyranopyrazoles using magnetic Fe_3O_4 nanoparticles as ef fi cient and reusable catalyst, 70 (2014) 2971–2975.
[30] B. Jaleh, A. Jabbari, Evaluation of reduced graphene oxide/ZnO effect on properties of PVDF nanocomposite films, *Appl. Surf. Sci.* 320 (2014) 339–347.
[31] A. Sotto, J. Kim, J.M. Arsuaga, G. del Rosario, A. Martinez, D. Nam, P. Luis, B. Van der Bruggen, Binary metal oxides for composite ultrafiltration membranes, *J. Mater. Chem. A* 2 (2014) 7054–7064.
[32] S.J. Oh, N. Kim, Y.T. Lee, Preparation and characterization of PVDF/TiO_2 organic-inorganic composite membranes for fouling resistance improvement, *J. Membr. Sci.* 345 (2009) 13–20.
[33] A. Nedzarek, A. Drost, F.B. Harasimiuk, A. Tórz, The influence of pH and BSA on the retention of selected heavy metals in the nanofiltration process using ceramic membrane, *Desalination* 369 (2015).
[34] D.K. Bora, P. Deb, Fatty acid binding domain mediated conjugation of ultrafine magnetic nanoparticles with albumin protein, *Nanoscale Res. Lett.* 4 (2009) 138–143.
[35] F. Adam, W.T. Ooi, Selective oxidation of benzyl alcohol to benzaldehyde over Co-metalloporphyrin supported on silica nanoparticles, *Appl. Catal. A Gen.* 445–446 (2012) 252–260.
[36] Y.Y. Yu, B. Lu, X.G. Wang, J.X. Zhao, X.Z. Wang, Q.H. Cai, Highly selective oxidation of benzyl alcohol to benzaldehyde with hydrogen peroxide by biphasic catalysis, *Chem. Eng. J.* 162 (2010).
[37] Y. Leng, J. Wang, P. Jiang, Amino-containing cross-linkedionic copolymer-anchored heteropoly acid for solvent-free oxidation of benzylalcohol with H_2O_2, *J. Catcom.* 27 (2012) 101–104.
[38] L.P. Kong, X.J. Gan, A.L. Bin Ahmad, B.H. Hamed, E.R. Evarts, B.S. Ooi, J.K. Lim, Design and synthesis of magnetic nanoparticles augmented microcapsule with catalytic and magnetic bifunctionalities for dye removal, *Chem. Eng. J.* 197 (2012) 350–358.
[39] M.G. Buonomenna, P. Macchi, M. Davoli, E. Drioli, Poly(vinylidene fluoride) membranes by phase inversion: the role the casting and coagulation conditions play in their morphology, crystalline structure and properties, *Eur. Polym. J.* 43 (2007) 1557–1572.